Proceedings Paper:
Ding, J, Zhou, C orcid.org/0000-0002-6677-0855, Guo, Z et al. (2 more authors) (2019) Versatile Reactive Bipedal Locomotion Planning Through Hierarchical Optimization. In: 2019 International Conference on Robotics and Automation (ICRA). 2019 International Conference on Robotics and Automation (ICRA), 20-24 May 2019, Montreal, QC, Canada. IEEE , pp. 256-262. ISBN 978-1-5386-8176-3

https://doi.org/10.1109/icra.2019.8794072

Versatile Reactive Bipedal Locomotion Planning Through Hierarchical Optimization

Jiatao Ding[1,2], Chengxu Zhou[2,3], Zhao Guo[1], Xiaohui Xiao[1], Nikos Tsagarakis[2]

***Abstract*— When experiencing disturbances during locomotion, human beings use several strategies to maintain balance, e.g. changing posture, modulating step frequency and location. However, when it comes to the gait generation for humanoid robots, modifying step time or body posture in real time introduces nonlinearities in the walking dynamics, thus increases the complexity of the planning. In this paper, we propose a two-layer hierarchical optimization framework to address this issue and provide the humanoids with the abilities of step time and step location adjustment, Center of Mass (CoM) height variation and angular momentum adaptation. In the first layer, times and locations of consecutive two steps are modulated online based on the current CoM state using the Linear Inverted Pendulum Model. By introducing new optimization variables to substitute the hyperbolic functions of step time, the derivatives of the objective function and feasibility constraints are analytically derived, thus reduces the computational cost. Then, taking the generated horizontal CoM trajectory, step times and step locations as inputs, CoM height and angular momentum changes are optimized by the second-layer nonlinear model predictive control. This whole procedure will be repeated until the termination condition is met. The improved recovery capability under external disturbances is validated in simulation studies.**

I. Introduction

The deployment of humanoid robots in real-world environments requires locomotion control performance that can demonstrate quick response to external disturbances and uncertainties. In theory, humanoids can, like human beings, make use of various balancing strategies, including ankle strategy, hip strategy, stepping strategy and upper-body posture modulation, to keep balance while walking. Our goal in this paper, is to develop a versatile and robust framework for bipedal walking/balancing, which could integrate multiple strategies in a unified way.

To avoid high computation burden caused by full-body dynamics optimization, simplified models have been proposed, among which the Linear Inverted Pendulum Model (LIPM) is widely used [1]. Based on the LIPM, feasible Center of Mass (CoM) trajectories have been generated using preview control [2], analytic solution [3] and other methods, which manipulate the Zero Moment Point (ZMP) within the support polygon. However, due to the limited size of the support polygon, this type of tracking controllers can hardly handle larger disturbances. Thus, with considering the feasibility constraints, the Model Predictive Control (MPC) framework is proposed in [4] and then is extended in [5] to deal with footstep adaption. Since then, using the stepping strategy, robust walking has been realized, such as work in [6]. However, the lack of considering other balancing recovery strategies, such as modifications of vertical CoM motion, angular momentum and step time, limits the humanoids' capabilities against large disturbances.

Research efforts were made for the vertical CoM motion to achieve more robust walking [7]–[9]. Brasseur et al. [10] limited the nonlinear part of the dynamic feasibility constraints between extreme values and proposed a linear MPC for gait generation with time-varying height trajectory. In [11], the constrained optimization problem was formulated as a quadratically constrained Nonlinear MPC (NMPC) problem and was solved fast by Sequential Quadratic Programming (SQP). Besides, momentum optimization has attracted more attention in recent years [12], [13]. Zhao et al. [14] proposed a hybrid phase-space method to realize dynamic walking on uneven terrain, based on centroidal momentum dynamics. To further enhance the robustness, step location adjustment, angular momentum change and vertical height variation were combined together in a unified MPC framework in [15] and [16], where the fixed height trajectories were used as an inputs. While variable vertical motion and angular momentum change provide additional controllability for stable walking, further improvements are still needed when facing larger tracking errors caused by external disturbances.

Changing the step time in real time is another effective strategy that human commonly use while walking under dynamic disturbances. Several works [17]–[19] modulated the step time online by solving a large Nonlinear Programming Problem (NLP), which requires heavy computation load. Maximo et al. [20] adopted a mixed-integer Quadratic Programming (QP) method for step duration optimization but increased the computational complexity. To reduce time cost, Hu et al. [21] proposed one sequential approach with optimizing two walking steps, but only obtained the sub-optimal results. Based on the Divergent Component of Motion (DCM) dynamics, Khadiv et al. [22] linearized the nonlinear term of step duration and then optimized the step time by only solving a QP problem. Yet, this approach focused on one step adjustment, which may make the planner reject disturbance in a quite aggressive way. Furthermore, Caron et al. [23] used timing adaptation to limit the swing foot acceleration. Rather than optimization, Castano et al. [24] proposed an analytic method to determine the future

[1]School of Power and Mechanical Engineering, Wuhan University, Wuhan, Hubei Province, P. R. China 430072. jtding@whu.edu.cn, guozhao@whu.edu.cn, xhxiao@whu.edu.cn.

[2]Humanoid and Human Centered Mechatronics Research Line, Istituto Italiano di Tecnologia, via Morego, 30, Genova, Italy 16163. name.surname@iit.it.

[3]School of Mechanical Engineering, University of Leeds, Leeds, UK.

step time based on current state and reference step locations. Yet, this work also took into consideration one step adaption. In [25], Ding et al. proposed another analytic method to adjust step time and step locations, which just obtained the feasible solution. Then, using instantaneous capture point dynamics, another fast method for step time determination was proposed in [26]. However, this approach is not effective enough when the push forces are not along the desired stepping direction.

In our previous work [27], based on the Inverted Pendulum plus a Flywheel Model (IPFM), we proposed a robust NMPC framework for bipedal gait generation which can deal with reactive stepping, variable vertical CoM motion and angular momentum adaptation simultaneously. In this paper, we aim to take into account also the online step time modulation to extend our gait generation framework.

For the sake of computational efficiency, the proposed framework generates the optimal pattern in a hierarchical manner by solving two optimization sub-problems iteratively. Firstly, using the LIPM, the step times and step locations of the current and next walking cycle are optimized simultaneously based on the current CoM state. By optimizing the step time related variables (introduced in following sections to substitute the hyperbolic functions of step time) rather than step time directly, high computation efficiency of the first NLP is achieved. Secondly, using the online-regenerated step locations, step times and CoM trajectory as inputs, the time-varying CoM height trajectory and upper-body inclination are then obtained by utilizing the NMPC framework proposed in [27]. Thus, the proposed hierarchical optimization strategy can optimize step time, step location, CoM height and upper-body inclination motions, based only on the reference gait parameters. Furthermore, by deriving the close-formed expressions of derivatives of the objective functions and feasibility constraints, these two NLPs can be solved online via SQP.

The rest of this paper is organized as follows. In Section II, the overall procedure of the proposed framework is introduced briefly. Then, in Section III, the first NLP for step time and step location optimization using LIPM dynamics is explained in detail. Then, a brief introduction of the second NLP (the NMPC for optimizing CoM height and upper-body inclination) is given in Section IV. In Section V, the simulation results are discussed. Finally, we draw the conclusions in Section VI.

II. Framework Overview

The overall framework of the proposed walking pattern generation approach is shown in Fig. 1. As can be seen in Fig. 1, the two cascaded NLPs are solved iteratively until satisfying the termination condition to obtain optimal step time, step locations, CoM trajectories and upper-body inclination angles.

Taking the reference step time and step locations as inputs, the first NLP will modulate them in real time and generate a nominal horizontal CoM trajectory, given the current robot states. Then, they will be passed to the second NLP (an NMPC framework proposed in [27]). With integrating the vertical CoM adaptation and upper-body inclination changes, the NMPC, using the IPFM, would generate step commands and reference trajectories for the humanoid robot.

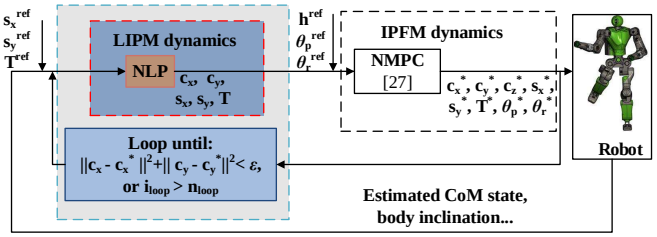

Fig. 1: Overview of the proposed framework.

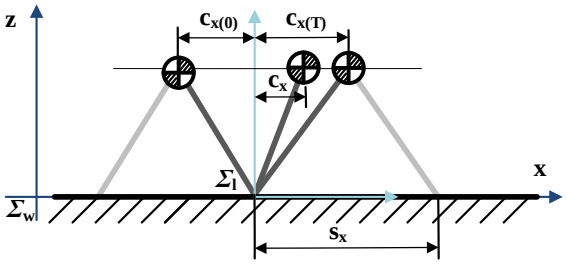

Fig. 2: LIPM motion in sagittal plane, $c_{x(0)}$ and $c_{x(T)}$ represent the initial and final CoM position relative to the current support center, respectively, s_x is the step length.

This procedure is repeated until the CoM trajectories generated by both NLPs eventually converge or the maximum iteration number is reached. Specifically, in this work, we found in most cases only one loop is enough for the algorithm to converge.

III. Optimization of Step Time and Step Location

A. LIPM dynamics

For the LIPM with constant CoM height, during each walking cycle, its dynamics described in support foot (the local coordinate) is shown as follows [1],

$$\ddot{c}_x = \omega^2 c_x, \quad \ddot{c}_y = \omega^2 c_y, \quad \omega = \sqrt{g/Z_c}, \tag{1}$$

where $[c_x, c_y]^T$ denote the position of CoM relative to the current support center (the fixed ZMP reference), Z_c is the fixed height of the LIPM, g and ω are the gravitational acceleration and natural frequency, respectively.

Taking the sagittal motion (shown in Fig. 2) as an example, the final CoM state of one walking cycle determined by (1) could be solved analytically, given the current state, by

$$\begin{aligned} c_{x(T)} &= c_{x(t_e)} \cosh(\omega(T-t_e)) + \frac{\dot{c}_{x(t_e)}}{\omega} \sinh(\omega(T-t_e)), \\ \dot{c}_{x(T)} &= c_{x(t_e)} \omega \sinh(\omega(T-t_e)) + \dot{c}_{x(t_e)} \cosh(\omega(T-t_e)), \end{aligned} \tag{2}$$

where t_e is the elapsed time of current step, T is the time period of the walking cycle, $[c_{x(t_e)}, \dot{c}_{x(t_e)}]^T$ and $[c_{x(T)}, \dot{c}_{x(T)}]^T$ are the current and the final CoM state, respectively.

Here, we introduce new step-time related variables

$$\begin{aligned} t_{ch} &= \cosh(\omega(T-t_e)), \\ t_{sh} &= \sinh(\omega(T-t_e)). \end{aligned} \tag{3}$$

As a result, (2) becomes to

$$\begin{aligned} c_{\mathrm{x}(T)} &= c_{\mathrm{x}(t_\mathrm{e})} t_{\mathrm{ch}} + \frac{\dot{c}_{\mathrm{x}(t_\mathrm{e})}}{\omega} t_{\mathrm{sh}}, \\ \dot{c}_{\mathrm{x}(T)} &= c_{\mathrm{x}(t_\mathrm{e})} \omega t_{\mathrm{sh}} + \dot{c}_{\mathrm{x}(t_\mathrm{e})} t_{\mathrm{ch}}. \end{aligned} \tag{4}$$

Since the two new variables defined in (3) decrease strictly when the elapsed time t_e increases from 0 to T, this change can simplify the constraints handling when solving the NLP. Furthermore, from (4), it can be seen that the final state has linear relationship with the new introduced variables t_{ch} and t_{sh}. Thus, the computational complexity is reduced and the NLP problem can be solved very fast.

B. NLP Formulation

When the actual state diverges from the reference state due to the external disturbances and uncertainties, it is necessary to update the walking patterns to bring the robot back to stable walking cycles. In this section, using the LIPM, the first NLP in our framework is formulated to optimize the step time and location simultaneously.

1) Objective Function: To drive robot to move from any initial state to the stable state, here we not only track the final CoM position and velocity references at the current step, but also consider one following step to improve the robustness. This strategy of planning future two-step will cover the most balancing recovery cases, according to [28] and [29]. By minimizing the errors between actual and desired step location, remaining step time, final CoM position and the final CoM velocity, the objective function at time t during the i^{th} walking cycle is formulated as follows,

$$f(\mathbf{X}) = \sum_{\mathbf{U}} \frac{\sigma_{\mathbf{U}}}{2} \parallel \mathbf{U} - \mathbf{U}^{\mathrm{ref}} \parallel^2, \tag{5}$$

where the optimization variable

$$\mathbf{X} = [{}^{i}s_{\mathrm{x}}, {}^{i}s_{\mathrm{y}}, {}^{i}t_{\mathrm{ch}}, {}^{i}t_{\mathrm{sh}}, {}^{i+1}s_{\mathrm{x}}, {}^{i+1}s_{\mathrm{y}}, {}^{i+1}t_{\mathrm{ch}}, {}^{i+1}t_{\mathrm{sh}}]^T$$

consists of the two consecutive steps' positions (s_{x}, s_{y}) and the step time related variables (t_{ch}, t_{sh}) introduced in (3). And

$$\mathbf{U} \in \{\mathbf{X}, {}^{i}c_{\mathrm{x}(T)}, {}^{i}c_{\mathrm{y}(T)}, {}^{i}\dot{c}_{\mathrm{x}(T)}, {}^{i}\dot{c}_{\mathrm{y}(T)}, {}^{i+1}c_{\mathrm{x}(T)}, {}^{i+1}c_{\mathrm{y}(T)}\}$$

forms the cost terms of the objective function, which evaluates the tracking errors of the CoM final states in the next two steps. Particularly, the final velocity of the $(i+1)^{\mathrm{th}}$ cycle is not included here to reduce the computational complexity. $\sigma_{\mathbf{U}}$ is the weight of the item in $\mathbf{U}$, which is set to be greater than zero so that Hessian matrix is positive-definite.

Notation $\{\}^{\mathrm{ref}}$ denotes the reference of each cost term. Specifically, the reference step parameters for the first step are determined by both the current states and pre-defined reference parameters while the references for consecutive next step are merely determined by the pre-defined parameters. For example, the ${}^{i}s_{\mathrm{x}}^{\mathrm{ref}}$, ${}^{i+1}s_{\mathrm{x}}^{\mathrm{ref}}$, ${}^{i}t_{\mathrm{ch}}^{\mathrm{ref}}$ and ${}^{i+1}t_{\mathrm{ch}}^{\mathrm{ref}}$ are given by,

$$\begin{cases} {}^{i}s_{\mathrm{x}}^{\mathrm{ref}} = {}^{i+1}d_{\mathrm{x}}^{\mathrm{ref}} - {}^{i}d_{\mathrm{x}}, & {}^{i+1}s_{\mathrm{x}}^{\mathrm{ref}} = {}^{i+2}d_{\mathrm{x}}^{\mathrm{ref}} - {}^{i+1}d_{\mathrm{x}}^{\mathrm{ref}}, \\ {}^{i}t_{\mathrm{ch}}^{\mathrm{ref}} = \cosh(\omega({}^{i}T^{\mathrm{ref}} - t_\mathrm{e})), & {}^{i+1}t_{\mathrm{ch}}^{\mathrm{ref}} = \cosh(\omega({}^{i+1}T^{\mathrm{ref}})), \end{cases} \tag{6}$$

where ${}^{i}d_{\mathrm{x}}$ represents the sagittal footstep location calculated by adding the generated step length, ${}^{i+1}d_{\mathrm{x}}^{\mathrm{ref}}$ and ${}^{i+2}d_{\mathrm{x}}^{\mathrm{ref}}$ represent the pre-defined sagittal foot locations calculated by adding the reference step length, ${}^{i}T^{\mathrm{ref}}$ and ${}^{i+1}T^{\mathrm{ref}}$ represent the pre-defined reference time duration of current step and next one step, respectively.

Furthermore, the usage of variables t_{ch} and t_{sh} rather than $(T - t_\mathrm{e})$ helps to derive the close-form of the derivative of objective function. For example, the cost term of tracking error of the final CoM position during the current step (${}^{i}c_{\mathrm{x}(T)}$ in $\mathbf{U}$) is given by,

$$\begin{aligned} f(\mathbf{X})_{{}^{i}c_{\mathrm{x}(T)}} &= \| {}^{i}c_{\mathrm{x}(T)} - {}^{i}c_{\mathrm{x}(T)}^{\mathrm{ref}} \|^2 = \| {}^{i}c_{\mathrm{x}(t_\mathrm{e})} {}^{i}t_{\mathrm{ch}} + \frac{\dot{c}_{\mathrm{x}(t_\mathrm{e})}}{\omega} {}^{i}t_{\mathrm{sh}} - \frac{{}^{i}s_{\mathrm{x}}^{\mathrm{ref}}}{2} \|^2 \\ &= \| (\mathbf{A} + \mathbf{B})^T \mathbf{X} - a \|^2, \end{aligned} \tag{7}$$

where the a denotes the constant ${}^{i}s_{\mathrm{x}}^{\mathrm{ref}}/2$, which is set to be ${}^{i}c_{\mathrm{x}(T)}^{\mathrm{ref}}$, the $\mathbf{A} \in \Re^8$ and $\mathbf{B} \in \Re^8$ are the constant coefficient matrices w.r.t variable ${}^{i}t_{\mathrm{ch}}$ and ${}^{i}t_{\mathrm{sh}}$, respectively, and are given by

$$\begin{cases} \mathbf{A} = [0, 0, c_{\mathrm{x}(t_\mathrm{e})}, 0, 0, 0, 0, 0]^T, \\ \mathbf{B} = [0, 0, 0, \dot{c}_{\mathrm{x}(t_\mathrm{e})}/\omega, 0, 0, 0, 0]^T. \end{cases} \tag{8}$$

As a result, the first and second order derivatives of this term are given analytically by

$$\begin{cases} \nabla_{\mathbf{x}}^2 (f(\mathbf{X})_{{}^{i}c_{\mathrm{x}(T)}}) = 2(\mathbf{A} + \mathbf{B})(\mathbf{A} + \mathbf{B})^T, \\ \nabla_{\mathbf{x}} (f(\mathbf{X})_{{}^{i}c_{\mathrm{x}(T)}}) = 2(\mathbf{A} + \mathbf{B})((\mathbf{A} + \mathbf{B})^T \mathbf{X} - a). \end{cases} \tag{9}$$

Specifically, the cost terms of tracking error of the ${}^{i+1}c_{\mathrm{x}(T)}$ and ${}^{i+1}c_{\mathrm{y}(T)}$ are the 4^{th} polynomial w.r.t corresponding optimization variables. However, the close-formed expressions of their derivatives can also be computed in the same way. Thus, this NLP can be solved fast by SQP.

2) Constraints: To guarantee the feasibility, this section describes the constraints of step time, step location and CoM state. All these constraints are expressed in quadratic forms, similar with [27].

Constraints of step time: The step frequency is determined by the step time, which is limited by the physical structure and actuation capability.

Firstly, given the lower boundary (T^{min}) and upper boundary (T^{max}) of step time, we can easily derive the constraints on variables t_{ch} and t_{sh} by utilizing the monotony of hyperbolic functions. For example, the linear constraint of t_{ch}

$$\begin{cases} \cosh(\omega(\max(T^{\mathrm{min}} - t_\mathrm{e}, 0))) \leq {}^{i}t_{\mathrm{ch}} \leq \cosh(\omega(T^{\mathrm{max}} - t_\mathrm{e})), \\ \cosh(\omega T^{\mathrm{min}}) \leq {}^{i+1}t_{\mathrm{ch}} \leq \cosh(\omega T^{\mathrm{max}}), \end{cases} \tag{10}$$

Additionally, following equality constraint should also be satisfied for the two steps,

$${}^{j}t_{\mathrm{ch}}^2 - {}^{j}t_{\mathrm{sh}}^2 = 1, j \in \{i, i+1\}. \tag{11}$$

Constraints of step location: Step locations, as the optimization variables, should meet feasibility limitations, such as maximal leg length, maximal joint velocities, self-collision avoidance etc. At the present, we only limit the step length and step width into a reasonable range. Taking the step

length for instance, the following constraints are introduced for the next two steps,

$$ {}^{j}s_{\mathrm{x}}^{\min} \leq s_{\mathrm{x}} \leq {}^{j}s_{\mathrm{x}}^{\max}, j \in \{i, i+1\}, \tag{12} $$

where $s_{\mathrm{x}}^{\min}$ and $s_{\mathrm{x}}^{\max}$ are the lower and upper boundaries of step length. Same constraints are also applied to step width.

Constraints of CoM acceleration: With solving this NLP, the robot's state is expected to converge from the current real state to the stable state. However, the cost term about the CoM acceleration variation is not incorporated into the objective function (5). Therefore, the generated CoM trajectory may demand strong actuation capability that goes beyond the physical limits. To avoid this, the CoM acceleration is constrained as

$$ \ddot{c}_{\mathrm{x}}^{\min} \leq \ddot{c}_{\mathrm{x}(t+\Delta t)} \leq \ddot{c}_{\mathrm{x}}^{\max}, \tag{13} $$

where Δt is the sampling time interval, $\ddot{c}_{\mathrm{x}(t+\Delta t)}$ denotes the generated CoM acceleration at next sampling time, $\ddot{c}_{\mathrm{x}}^{\min}$ and $\ddot{c}_{\mathrm{x}}^{\max}$ are the lower and upper boundary of CoM acceleration, respectively, which are determined by the maximal joint torques.

IV. NMPC Framework Exploiting Angular Momentum and CoM Height Changes

After determining the step parameters using the first NLP, a NMPC approach is integrated to exploit the angular momentum and CoM height adaptation. The NMPC has been validated in our previous work [27], which is introduced briefly in this section.

A. IPFM Dynamics

The LIPM, assuming a lumped mass body and the constant CoM height, limits the robot's performance undergoing external perturbations. The IPFM, assuming a flywheel with rotational inertia and allowing the 3D CoM motion, can be used to model angular momentum change and vertical body motion. The ZMP, that must be inside the robot's support polygon, of the IPFM can be calculated by

$$ p_{\mathrm{x}} = c_{\mathrm{x}}^{\mathrm{w}} - \frac{c_{\mathrm{z}}^{\mathrm{w}} - d_{\mathrm{z}}}{g + \ddot{c}_{\mathrm{z}}^{\mathrm{w}}} \ddot{c}_{\mathrm{x}}^{\mathrm{w}} - \frac{\dot{L}_{\mathrm{y}}}{m(g + \ddot{c}_{\mathrm{z}}^{\mathrm{w}})}, \dot{L}_{\mathrm{y}} = I_{\mathrm{y}} \ddot{\theta}_{\mathrm{p}}, \tag{14} $$

$$ p_{\mathrm{y}} = c_{\mathrm{y}}^{\mathrm{w}} - \frac{c_{\mathrm{z}}^{\mathrm{w}} - d_{\mathrm{z}}}{g + \ddot{c}_{\mathrm{z}}^{\mathrm{w}}} \ddot{c}_{\mathrm{y}}^{\mathrm{w}} + \frac{\dot{L}_{\mathrm{x}}}{m(g + \ddot{c}_{\mathrm{z}}^{\mathrm{w}})}, \dot{L}_{\mathrm{x}} = I_{\mathrm{x}} \ddot{\theta}_{\mathrm{r}}, \tag{15} $$

where $[p_{\mathrm{x}}, p_{\mathrm{y}}, p_{\mathrm{z}}]^T$,$[c_{\mathrm{x}}^{\mathrm{w}}, c_{\mathrm{y}}^{\mathrm{w}}, c_{\mathrm{z}}^{\mathrm{w}}]^T$ and $[d_{\mathrm{x}}, d_{\mathrm{y}}, d_{\mathrm{z}}]^T$ denote the global position of ZMP, CoM and supporting foot, respectively, L_{x} and L_{y}, I_{x} and I_{y}, θ_{r} and θ_{p} denote angular momentum, moment of inertia and flywheel rotation angle about x- and y-axis, respectively, m is the overall mass.

B. NMPC Problem Formulation

1) Objective Function: At time t, the objective function for the second NLP is defined as follows,

$$ \begin{aligned} f = \sum_{\mathbf{Q}}^{\mathbf{C}_{\mathrm{x}}, \mathbf{C}_{\mathrm{y}}, \mathbf{C}_{\mathrm{z}}, \mathbf{\Theta}_{\mathrm{r}}, \mathbf{\Theta}_{\mathrm{p}}} \Big\{ \frac{\alpha_{\mathbf{Q}}}{2} \parallel \dot{\mathbf{Q}} \parallel^2 + \frac{\beta_{\mathbf{Q}}}{2} \parallel \mathbf{Q} - \mathbf{Q}^{\mathrm{ref}} \parallel^2 \\ + \frac{\gamma_{\mathbf{Q}}}{2} \parallel \ddot{\mathbf{Q}} \parallel^2 \Big\} + \sum_{\mathbf{V}}^{\mathbf{D}_{\mathrm{x}}, \mathbf{D}_{\mathrm{y}}, \mathbf{D}_{\mathrm{z}}} \frac{\delta_{\mathbf{V}}}{2} \parallel \mathbf{V} - \mathbf{V}^{\mathrm{ref}} \parallel^2, \end{aligned} \tag{16} $$

TABLE I: Algorithm parameters for the first NLP

$\sigma_{i_{c_{\mathrm{x}(T)}}}$	5×10^6	$\sigma_{i_{c_{\mathrm{y}(T)}}}$	5×10^6
$\sigma_{i_{s_{\mathrm{x}}}}$	5×10^7	$\sigma_{i_{s_{\mathrm{y}}}}$	5×10^7
$\sigma_{i_{t_{\mathrm{ch}}}}$	5×10^9	$\sigma_{i_{t_{\mathrm{sh}}}}$	5×10^9
$\sigma_{i+1_{c_{\mathrm{x}(T)}}}$	1×10^2	$\sigma_{i+1_{c_{\mathrm{y}(T)}}}$	1×10^2
$\sigma_{i+1_{s_{\mathrm{x}}}}$	10	$\sigma_{i+1_{s_{\mathrm{y}}}}$	10
$\sigma_{i+1_{t_{\mathrm{ch}}}}$	1×10^3	$\sigma_{i+1_{t_{\mathrm{sh}}}}$	1×10^3
$\sigma_{i_{\dot{c}_{\mathrm{x}(T)}}}$	1×10^3	$\sigma_{i_{\dot{c}_{\mathrm{y}(T)}}}$	1×10^3
Δt[s]	0.05	$g[\mathrm{m\cdot s^{-2}}]$	9.8

TABLE II: Parameters for constraints of the first NLP

Step location constraints		$T_{\mathrm{x}}^{\max}$[s]	2
$s_{\mathrm{x}}^{\min}$[m]	0	CoM acceleartion constraints	
$s_{\mathrm{x}}^{\max}$[m]	0.6	$\ddot{c}_{\mathrm{x}}^{\min}[\mathrm{m\cdot s^{-2}}]$	-13
$s_{\mathrm{y}}^{\min}$[m]	0.2	$\ddot{c}_{\mathrm{x}}^{\max}[\mathrm{m\cdot s^{-2}}]$	13
$s_{\mathrm{y}}^{\max}$[m]	0.6	$\ddot{c}_{\mathrm{y}}^{\min}[\mathrm{m\cdot s^{-2}}]$	-12
Step constraints		$\ddot{c}_{\mathrm{y}}^{\max}[\mathrm{m\cdot s^{-2}}]$	12
$T_{\mathrm{x}}^{\min}$[s]	0.6	/	/

where $\mathbf{Q} \in \{\mathbf{C}_{\mathrm{x}}, \mathbf{C}_{\mathrm{y}}, \mathbf{C}_{\mathrm{z}}, \mathbf{\Theta}_{\mathrm{r}}, \mathbf{\Theta}_{\mathrm{p}}\}$ represent the future trajectories of CoM along x-, y- and z- axis, and the upper-body inclination angle about x- and y- axis, respectively, $\mathbf{V} \in \{\mathbf{D}_{\mathrm{x}}, \mathbf{D}_{\mathrm{y}}, \mathbf{D}_{\mathrm{z}}\}$ represent the future step locations during the prediction horizon. Please refer to [27] for more details.

A major difference with [27] is that, instead of directly setting support foot centers to be the reference horizontal CoM trajectory (the $\mathbf{C}_{\mathrm{x}}^{\mathrm{ref}}$ and $\mathbf{C}_{\mathrm{y}}^{\mathrm{ref}}$ used in (16)), in this paper, the nominal reference CoM trajectory is generated by the first NLP. Besides, the reference step location (except step height) and step time are also generated by the first NLP. These features help to reduce the time cost of the NMPC loop and as well improve the ZMP tracking performance, which would be discussed in details in following sections.

2) Constraints: To guarantee the feasibility, we take into account the constraints of ZMP movement (calculated by (14) and (15)), footstep location, CoM vertical motion, upper-body inclination and joint torques. Furthermore, these constraints are expressed in quadratic forms. For more details, please refer to [27].

V. Simulation Validations

In this section, we first validate the whole framework by generating 3D walking pattern with variable step parameters, using the physical specifications of the CogIMon humanoid robot [30]. Then, we demonstrate the improved capability for balance recovery with the step time modulation. The simulation parameters for the first NLP are listed in Table I and Table II and the parameters for the second NLP are the same with [27].

A. 3D Walking with Variant Step Parameters

With the step parameters listed in Table III, the 3D walking pattern was generated. In this section, the reference step time is 0.8 s, and the relative CoM height reference (w.r.t support foot) is 1.02 m.

TABLE III: Step parameters for 3D walking

Parameters \ steps	1	2-4	5	6	7-
step length (s_x[m])	0	0.3	0.1	0.6	0.3
step width (s_y[m])	0.2	0.4	0.2	0.6	0.4
step height (s_z[m])	0	0.1	0.1	-0.1	-0.1

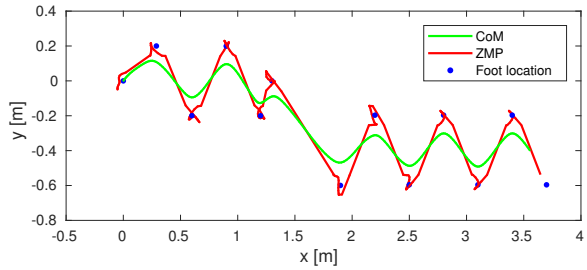

Fig. 3: Generated CoM trajectory, ZMP trajectory and footstep locations for 3D walking.

As can be seen in Fig. 3, the feasible 3D gait as well as the smooth CoM height trajectory was successfully generated by the proposed framework. That is to say, the time-varying vertical CoM motion was generated without strictly following the pre-defined reference trajectory when walking on the uneven terrain. Furthermore, the upper-body also rotated slightly to maintain balance, as shown in Fig. 4.

Seen from Fig. 5, the generated ZMP trajectory remained within the supporting polygon even when walking from the 5^{th} step to the 6^{th} with severe change of step parameters as listed in Table III. When walking back with constant step parameters, the ZMP trajectory stayed near the support center, which is different from our previous work [27], where the ZMP trajectory diverged to the edge of the support polygon. Thus, this work improves the ZMP tracking performance and

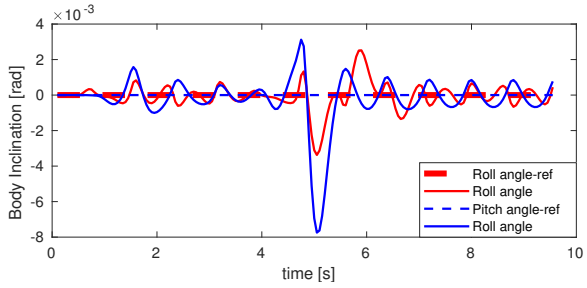

Fig. 4: Body inclination angles for 3D walking.

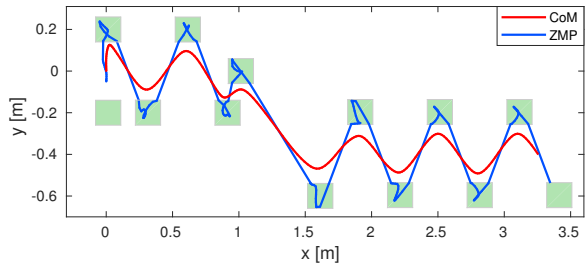

Fig. 5: Horizontal CoM trajectory, ZMP trajectory and footstep locations for 3D walking.

TABLE IV: Online-regenerated step parameters under external push ($s_x^{\text{ref}} = 0.3$ m, $s_y^{\text{ref}} = 0.4$ m $T^{\text{ref}} = 0.8$ s)

Parameters \ steps		2	3	4	5
s_x[m]	[27]	0.298	0.523	0.081	0.300
	this work	0.302	0.298	0.300	0.300
s_y[m]	[27]	0.414	0.530	0.525	0.401
	this work	0.400	0.387	0.399	0.399
T[s]	[27]	0.800	0.800	0.800	0.800
	this work	0.800	0.762	0.800	0.800

enhances the walking stability. This is because that, in this paper, the reference CoM trajectory for the NMPC is defined by the nominal CoM trajectory generated by the first NLP, rather than as the support center as done in previous work.

B. Balance Recovery from External Pushes

In this section, we compare the recovery capability of this work (with step time adjustment) with that of our previous work (without step time adjustment) under external push when tracking the same step locations. The external forces along x- axis and y- axis applied to the robot at 2 s, and lasted for 0.5 s.

Under the same external force (forward 160 N, lateral 120 N), the optimized step parameters are listed in Table IV. Moreover, other results such as horizontal CoM and ZMP trajectories, body inclinations and CoM heights are compared in Fig. 6-8.

The reference step length and width were 0.3 m and 0.4 m, and the reference step cycle was 0.8 s for both strategies. As can be seen in Table IV, when using the proposed framework in this paper, the step time is updated in real time. When the external push was applied, the step time was decreased to 0.762 s to keep balance. As a result, smaller changes of step length and step width were needed. Without step time adjustment, the step length and step width changed to be 0.523 m and 0.530 m, which resulted in a severer variation when compared with 0.298 m and 0.387 m in this work. This phenomenon can also be seen from Fig. 6, meaning that, when walking in the narrow space where the step location adjustment is limited, the proposed framework will take more advantage because it can turn to modulate the step time to compensate for disturbances.

Again, as seen in Fig. 6, when the robot returned back to the normal gait, the ZMP trajectory generated by the previous work [27] diverged from the support center to the edge of the support edge. However, in this work, the ZMP trajectory stayed closer to the support center, which helps to enhance the stability.

As expected, the required body inclination and vertical motion were also reduced dramatically, as shown in Fig. 7 and Fig. 8.

Further analysis reveals that, the integration of step time adjustment can reject larger external pushes. As listed in Table V, the previous work [27] could only reject 180 N forward force and 150 N lateral force, while this work can withstand 390 N forward force and 310 N lateral force.

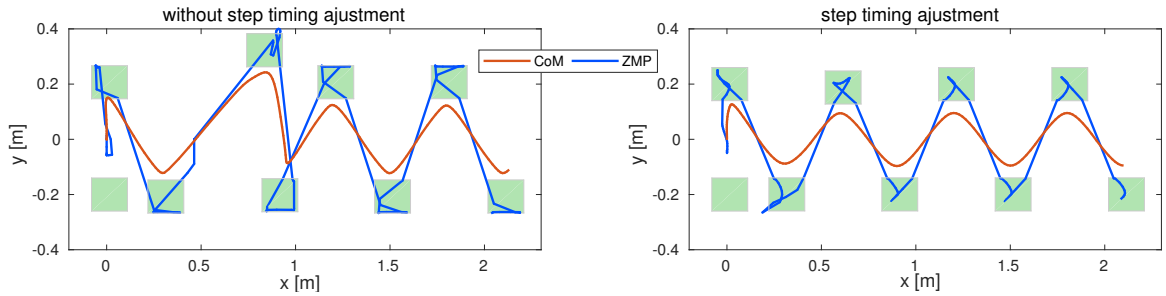

Fig. 6: Generated CoM trajectory, ZMP trajectory and footstep locations using different strategies when faced with external push, the green blocks represent the footstep locations.

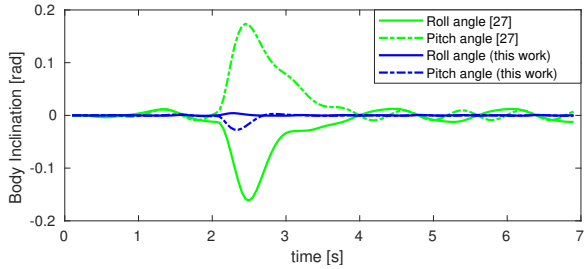

Fig. 7: Body inclination angles generated by different strategies.

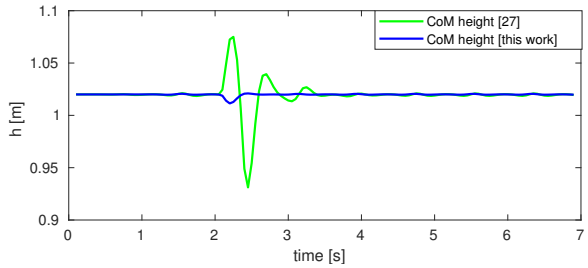

Fig. 8: Vertical height trajectories generated by different strategies.

C. Computation Efficiency

In this paper, by introducing the step time related variable for the first NLP, the close-formed derivatives of the objective function and constraints can be computed easily. As a result, the NLP can be solved fast by SQP, which is also used for solving the NPMC in [27].

To solve these two NLPs, the C++ optimization library *QuadProg++*, available under GNU General Public License, is used. Depending on the initial conditions, the time cost of each loop will vary much. However, the time cost of the first NLP is less than 60 us on a 3.0 GHz quad-core CPU. Since the reference horizontal CoM trajectory and the reference step locations for the second NMPC are already calculated by the first-layer NLP, the prediction horizon of the NMPC was reduced to be 1.05 s. Additionally, since the nominal CoM state serves as the warm-start, the maximal number of the SQP loop for the NMPC was reduced to be 2. As the result, the time cost of the second NMPC is reduced to be less than 5.5 ms. That is to say, compared with [27], the framework proposed here dramatically enhances the capability of balance recovery with almost no increasing the computation burden. Most importantly, the time cost for the whole-algorithm here is less than 6 ms, thus meets the requirement for hardware application.

TABLE V: Maximal external forces the robot can reject with/without step time change

Force \ Strategy	previous work [27]	this work
Forward force [N]	180	390
Lateral force [N]	150	310

VI. Conclusion

In this paper, we proposed a versatile and robust framework for walking pattern generation. Using the hierarchical optimization approach, the framework can exploit the step location and step time adjustment, angular momentum adaptation and vertical height variation in an unified way.

For step location and step time optimization, the LIPM is used. Tracking the reference step parameters and CoM state, the objective function is established. By substituting the optimal variables, we derive the close-formed expressions of NLP and solved it by SQP. By integrating the previously proposed NMPC in one loop, the robot achieved higher adaptability under 3D terrain and improved capability for balance recovery from external disturbances.

Acknowledgement

This work is supported by National Natural Science Foundation of China (Grant No. 51675385) and European Union's Horizon 2020 robotics program CogIMon (ICT-23-2014, 644727). Besides, the first author is also funded by China Scholarship Council (CSC).

References

[1] S. Kajita, F. Kanehiro, K. Kaneko, K. Yokoi, and H. Hirukawa, "The 3d linear inverted pendulum mode: A simple modeling for a biped walking pattern generation," in *IEEE/RSJ International Conference on Intelligent Robots and Systems*, vol. 1, 2001, pp. 239–246.

[2] S. Kajita, F. Kanehiro, K. Kaneko, K. Fujiwara, K. Harada, K. Yokoi, and H. Hirukawa, "Biped walking pattern generation by using preview control of zero-moment point," in *IEEE International Conference on Robotics and Automation*, vol. 2, 2003, pp. 1620–1626.

[3] K. Harada, S. Kajita, K. Kaneko, and H. Hirukawa, "An analytical method for real-time gait planning for humanoid robots," *International Journal of Humanoid Robotics*, vol. 3, no. 01, pp. 1–19, 2006.

[4] P.-B. Wieber, "Trajectory free linear model predictive control for stable walking in the presence of strong perturbations," in *IEEE-RAS International Conference on Humanoid Robots*, 2006, pp. 137–142.

[5] H. Diedam, D. Dimitrov, P.-B. Wieber, K. Mombaur, and M. Diehl, "Online walking gait generation with adaptive foot positioning through linear model predictive control," in *IEEE/RSJ International Conference on Intelligent Robots and Systems*, 2008, pp. 1121–1126.

[6] S. Feng, X. Xinjilefu, C. G. Atkeson, and J. Kim, "Robust dynamic walking using online foot step optimization," in *IEEE/RSJ International Conference on Intelligent Robots and Systems*, 2016, pp. 5373–5378.

[7] J. Englsberger, C. Ott, and A. Albu-Schäffer, "Three-dimensional bipedal walking control based on divergent component of motion," *IEEE Transactions on Robotics*, vol. 31, no. 2, pp. 355–368, 2015.

[8] Y. Liu, P. M. Wensing, J. P. Schmiedeler, and D. E. Orin, "Terrain-blind humanoid walking based on a 3-d actuated dual-slip model," *IEEE Robotics and Automation Letters*, vol. 1, no. 2, pp. 1073–1080, 2016.

[9] S. Caron and A. Kheddar, "Dynamic walking over rough terrains by nonlinear predictive control of the floating-base inverted pendulum," in *IEEE/RSJ International Conference on Intelligent Robots and Systems*, 2017, pp. 5017–5024.

[10] C. Brasseur, A. Sherikov, C. Collette, D. Dimitrov, and P.-B. Wieber, "A robust linear mpc approach to online generation of 3d biped walking motion," in *IEEE-RAS International Conference on Humanoid Robots*, 2015, pp. 595–601.

[11] K. Van Heerden, "Real-time variable center of mass height trajectory planning for humanoids robots," *IEEE Robotics and Automation Letters*, vol. 2, no. 1, pp. 135–142, 2017.

[12] H. Dai, A. Valenzuela, and R. Tedrake, "Whole-body motion planning with centroidal dynamics and full kinematics," in *IEEE-RAS International Conference on Humanoid Robots*, 2014, pp. 295–302.

[13] G. Wiedebach, S. Bertrand, T. Wu, L. Fiorio, S. McCrory, R. Griffin, F. Nori, and J. Pratt, "Walking on partial footholds including line contacts with the humanoid robot atlas," in *IEEE-RAS International Conference on Humanoid Robots*, 2016, pp. 1312–1319.

[14] Y. Zhao, B. R. Fernandez, and L. Sentis, "Robust optimal planning and control of non-periodic bipedal locomotion with a centroidal momentum model," *The International Journal of Robotics Research*, vol. 36, no. 11, pp. 1211–1242, 2017.

[15] J. Lack, "Integrating the effects of angular momentum and changing center of mass height in bipedal locomotion planning," in *IEEE-RAS International Conference on Humanoid Robots*, 2015, pp. 651–656.

[16] M. Shafiee-Ashtiani, A. Yousefi-Koma, and M. Shariat-Panahi, "Robust bipedal locomotion control based on model predictive control and divergent component of motion," in *IEEE International Conference on Robotics and Automation*, 2017, pp. 3505–3510.

[17] Z. Aftab, T. Robert, and P.-B. Wieber, "Ankle, hip and stepping strategies for humanoid balance recovery with a single model predictive control scheme," in *IEEE-RAS International Conference on Humanoid Robots*, 2012, pp. 159–164.

[18] C. Zhou, X. Wang, Z. Li, and N. Tsagarakis, "Overview of Gait Synthesis for the Humanoid COMAN," *Journal of Bionic Engineering*, vol. 14, no. 1, pp. 15–25, 2017.

[19] P. Kryczka, P. Kormushev, N. G. Tsagarakis, and D. G. Caldwell, "Online regeneration of bipedal walking gait pattern optimizing footstep placement and timing," in *IEEE/RSJ International Conference on Intelligent Robots and Systems*, 2015, pp. 3352–3357.

[20] M. R. Maximo, C. H. Ribeiro, and R. J. Afonso, "Mixed-integer programming for automatic walking step duration," in *IEEE/RSJ International Conference on Intelligent Robots and Systems*, 2016, pp. 5399–5404.

[21] W. Hu, I. Chatzinikolaidis, K. Yuan, and Z. Li, "Comparison study of nonlinear optimization of step durations and foot placement for dynamic walking," *arXiv preprint arXiv:1805.02155*, 2018.

[22] M. Khadiv, A. Herzog, S. A. A. Moosavian, and L. Righetti, "A robust walking controller based on online step location and duration optimization for bipedal locomotion," *arXiv preprint arXiv:1704.01271*, 2017.

[23] S. Caron and Q.-C. Pham, "When to make a step? tackling the timing problem in multi-contact locomotion by topp-mpc," in *IEEE-RAS International Conference on Humanoid Robotics*, 2017, pp. 522–528.

[24] J. A. Castano, Z. Li, C. Zhou, N. Tsagarakis, and D. Caldwell, "Dynamic and reactive walking for humanoid robots based on foot placement control," *International Journal of Humanoid Robotics*, vol. 13, no. 02, p. 1550041, 2016.

[25] J. Ding, Y. Wang, M. Yang, and X. Xiao, "Walking stabilization control for humanoid robots on unknown slope based on walking sequences adjustment," *Journal of Intelligent & Robotic Systems*, vol. 90, no. 3-4, pp. 323–338, 2018.

[26] R. J. Griffin, G. Wiedebach, S. Bertrand, A. Leonessa, and J. Pratt, "Walking stabilization using step timing and location adjustment on the humanoid robot, atlas," *arXiv preprint arXiv:1703.00477*, 2017.

[27] J. Ding, C. Zhou, S. Xin, X. Xiao, and N. Tsagarakis, "Nonlinear model predictive control for robust bipedal locomotion exploring com height and angular momentum changes," *arXiv preprint arXiv:1902.06770*, 2019.

[28] T. Koolen, T. De Boer, J. Rebula, A. Goswami, and J. Pratt, "Capturability-based analysis and control of legged locomotion, part 1: Theory and application to three simple gait models," *The International Journal of Robotics Research*, vol. 31, no. 9, pp. 1094–1113, 2012.

[29] P. Zaytsev, S. J. Hasaneini, and A. Ruina, "Two steps is enough: no need to plan far ahead for walking balance," in *IEEE International Conference on Robotics and Automation*, 2015, pp. 6295–6300.

[30] C. Zhou and N. Tsagarakis, "On the Comprehensive Kinematics Analysis of a Humanoid Parallel Ankle Mechanism," *ASME Journal of Mechanisms and Robotics*, 2018.